ORIGINAL ARTICLE

lajss.org Latin American Journal of Solids and Structures

www.lajss.org

Modeling and Experimental Validation of Two Adjacent Portal Frame Structures Subjected to Vibro-impact

Marcus V. M. Varanis [a,b*]

Arthur G. Mereles [a]

Anderson L. Silva [a]

Jose M. Balthazar [b,c]

Angelo M. Tusset [c]

Clivaldo Oliveira [a]

[a] Universidade Federal da Grande Dourados (UFGD), Dourados-MS, Brasil. E-mail: marcusvaranis@ufgd.edu.br, arthur_guilherme_mereles@hotmail.com, anderson.langone@outlook.com, clivaldoOliveira@ufgd.edu.br
[b] Faculdade de Engenharia de Bauru (Unesp), Bauru-SP, Brasil. E-mail: jmbaltha@gmail.com
[c] Universidade Tecnológica Federal do Paraná (UTFPR), Ponta Grossa - PR, Brasil. E-mail: a.m.tusset@gmail.com

*Corresponding author

http://dx.doi.org/10.1590/1679-78255435

Abstract

In many engineering applications, there are systems that exhibit a series of collisions in a certain amount of time, for example the impact of floating ice in ships and the rubbing between stationary and rotary parts in turbomachinery. In many of these situations, it is of vital importance to know how the impacts affect the overall system behavior for the correct functioning or the prediction of faults in the system. This can be done by proposing models that can represent the system when it is subjected to sudden impacts in its oscillation movement. However, due to the nonlinear and non-smooth characteristic of the impact phenomenon, the implementation of impacts in mechanical systems may be a challenging task. In this manner, this paper aims in proposing a vibro-impact model of two adjacent portal frame structures, being one of them driven by an unbalanced DC motor positioned on top of it. The portal frames were modeled as continuous beams by means of the Euler-Bernoulli beam theory. In order to model the impact between the structures, three different models were considered: using the Hertz theory of elastic bodies to model the contact force using a nonlinear damping; using a spring and a damper in parallel, viscoelastic or spring-dashpot system, to model the force; and considering the impact to be instantaneous and using the coefficient of restitution to adjust the velocity after the contact. To validate the impact models, an experimental procedure was performed and the measurements compared with the simulations.

Keywords

Vibro-impact, nonlinear model, Euler-Bernoulli theory, numeric simulations, experimental validation.

1 INTRODUCTION

Impact phenomena has been largely studied, since it is present in a great number of practical situations. This phenomenon is known for its intrinsic complexity, which makes its modeling a very challenging task. In the study of impact, there is one class of problems in which multiple impacts are seen in a certain amount of time. These systems are generally defined as vibro-impact systems and are seen in a large number of repeated engineering applications such as

Received: December 15, 2018. In Revised Form: February 22, 2019. Accepted: March 03, 2019. Available online: March 18, 2019.
http://dx.doi.org/10.1590/1679-78255435

response of heat exchanger tubes to aerodynamic excitation, impact of floating ice with ships, seismic pounding between buildings (Shi et al., 2018), slamming of ocean waves on off-shore against structures, ships colliding against fenders, rubbing between the stator structure and rotor blades in turbomachinery (Choy et al., 1988), hand-held percussion machines, among others (Ibrahim, 2009). One characteristic that is seen in impacting systems and can lead complicated vibration phenomena is the non-smoothness, which is the sudden change in the velocities of to the contacting bodies after the impact due to the high accelerations that they are subjected. This non-smoothness together with the nonlinear features of the impact phenomenon have to be accounted in the vibration modeling of it, so that one can make predictions of the vibro-impact systems (Ibrahim, 2009). In most cases, the motion of vibro-impact systems are very complex due to the non-smooth characteristic resulting from impact. Thus, they systems are commonly modeled using non-smooth differential equations. This modeling generally such as considers two situations for the system: with and without contact, which can be treated separately in most cases. A comprehensive review of impact modeling is presented in Gilardi and Sharf (2002). In Varanis et al. (2017) a review of models applied to vehicle crash by analysis is presented.

Two approaches are generally followed in the modeling of impact: considering the impacting bodies as rigid and the contact to be instantaneous, and formulating a force-deformation relation to account for the deformations of the bodies. The firsts models of impact were based in the hard collision hypothesis, which considers that the configurations impacting bodies is not changed significantly after the contact. In this approach, commonly defined as hard impact or impulse-momentum methods, the analysis of the collision is divided in the before and after impact, which are related by means of various coefficients, where the coefficient of restitution (COR) and the impulse ratio are the most employed ones (Brach, 1998). The COR depends on various parameters, such as the bodies' geometries, the impacting or approach velocity, the mechanical properties, the duration of the contact, and others. The dependence of the COR on the approach velocity can be explained considering the ratio between the time of contact and the natural period of vibration of the impacting bodies, this ratio is associated with the energy dissipation due to the elastic waves propagation. In case when this ratio is high, the COR is determined by the plastic deformations near the impact point, which extension is determined by the impacting velocity (Gilardi and Sharf, 2002). Some examples of studies considering hard impacts are presented in Wagg and Bishop (2000); Kobrinskij (1964); Peterka (1981); Pfeiffer (1987); Papadrakakis et al. (1991); Zhang et al. (2018). This approach, in spite of being simple and easy implemented in some cases, is unable to model systems with large contact time, as well as impact with deformed bodies.

Another approach used in the modeling of vibro-impacts systems consists in introducing a function to model the deformation of the impacting bodies during their contact. These are called soft impact or compliance models, and they model the phenomenon with more accuracy than the models based on hard impacts, since in the former the contact force takes a finite value and the contact time is not instantaneous. In this approach, the contact force is represented as a spring and a damping component to represent the stiffness and energy dissipation, respectively. In addition, the parameters used to represent the stiffness and the damping in the soft impact models are both related to the stiffness and damping coefficients, respectively. In case of simple contact between two bodies, the stiffness coefficient is mainly determined by the geometry and material properties of the impacting bodies, and the damping parameter can be related to the coefficient of restitution (Gilardi and Sharf, 2002). Some works that treated soft impact models are presented in Shaw and Holmes (1983); Aoki and Watanabe (1997); Lok and Wiercigroch (1996); Wiercigroch and Sin (1998); Peterka and Tondl (2004); Mereles et al. (2017b).

An important function used to represent soft impacts is obtained through the Hertz contact theory, which is an elastostatic theory used to calculate deformations of the bodies. This model, however did not account for the energy loss in the impact, as there was not a damping element in it. The first attempt to introduce damping in the Hertz model was performed by Dubowsky and Freudenstein (1971), where a linear damping element was utilized together with the Hertz nonlinear spring to model a system with compliance. This linear damping model did not represent the contact well enough, as shown by Hunt and Crossley (1975), since the model predicted a non-zero contact force at the beginning of the compression phase and a negative value at the separation phase. A more adequate model, according to Hunt and Crossley (1975), needed to give a nonlinear deformation-dependent damping force. Some applications of the Hertz force law in vibro-impact systems are presented in Pust and Peterka (2003); Muthukumar and DesRoches (2006); Pust (1999); Serweta et al. (2014); Navarro et al. (2014); Mereles et al. (2017a); Varanis et al. (2018b); Mereles et al. (2018).

Vibro-impact systems are known to present a great variety of vibration phenomena, such as chaotic motion, due to their strongly nonlinear characteristics. In the literature, many works concerned in the study of the dynamic behavior of vibro-impact systems can be found. For some examples, in Moraes et al. (2013) the dynamics of a vibro-impact system driven by ideal and non-ideal excitations is studied by means of time histories, phase portraits and frequency diagrams; the system presented chaotic behavior for certain vibration parameters. In Wang et al. (2013), a single-degree-of-freedom system impacting a hard barrier is studied and chaotic motion is revealed through time history diagram, phase

trajectory map, and Poincaré map; the system is then controlled by the method of controlling chaos by external periodic force feedback. Also, in Hiwarkar et al. (2011), the dynamics of a cantilever cracked bar is studied, the effect of contact nonlinearity due to crack's faces interaction is considered; the analysis showed nonlinear resonant phenomena due to vibro-impact interaction in the cracked bar. An experimental work is presented in Aguiar and Weber (2012), where a pendulum subjected to impacts is mounted on a moving cart which oscillated in different excitation frequencies; the nonlinear mathematical model showed rich responses and chaos and was validated by experimental data.

In this paper, the dynamics of a mechanical system consisting of two shear-building structures subjected to impacts is studied. The structures were modeled as a continuous system using the Euler-Bernoulli beam theory and the contact was modeled using different contact models. The shear-building structures are positioned side by side, being one of them driven by an unbalanced DC motor. In order to evaluate the model proposed, their responses were compared with signals obtained from an experimental procedure.

The work is divided as follows: Section 2 presents the mechanical system studied (Subsection 2.1) and the methods used to model the impacts (Subsections 2.2-2.4); in Section 3 the experimental setup is shown and described; the main impact parameters are obtained in Section 4; the results of the simulations and measurements are discussed in Section 6 and the conclusions are outlined in Section 6.

2 BACKGROUND

2.1 Vibro-impact model

The mechanical system consists of two portal frame structures which were modeled as continuous beams clamped at one end and with tip masses at the other. In order to study the vibro-impact phenomenon, an unbalanced DC motor, with an unbalance mass of m_u and a distance to the rotating axis of e, was placed on top of one of the structures, which were separated by a distance d, as depicted in Figure 1. The beams have the same length denoted by L, which was the impacting point considered. The displacements of the structures are given by $w(x,t)$ and $v(x,t)$. The equations of motion for the beams according to the Euler-Bernoulli beam theory are given by,

$$E_1 I_1 \frac{\partial^4 w}{\partial x^4}(x,t) + \rho_1 A_1 \frac{\partial^2 w}{\partial t^2}(x,t) + c_1 \frac{\partial w}{\partial t}(x,t) = \delta_d(x-L) m_u e\omega^2 \cos(\omega t) - \delta_d(x-L) F_c(t) \tag{2.1}$$

$$E_2 I_2 \frac{\partial^4 v}{\partial x^4}(x,t) + \rho_2 A_2 \frac{\partial^2 v}{\partial t^2}(x,t) + c_2 \frac{\partial v}{\partial t}(x,t) = \delta_d(x-L) F_c(t) \tag{2.2}$$

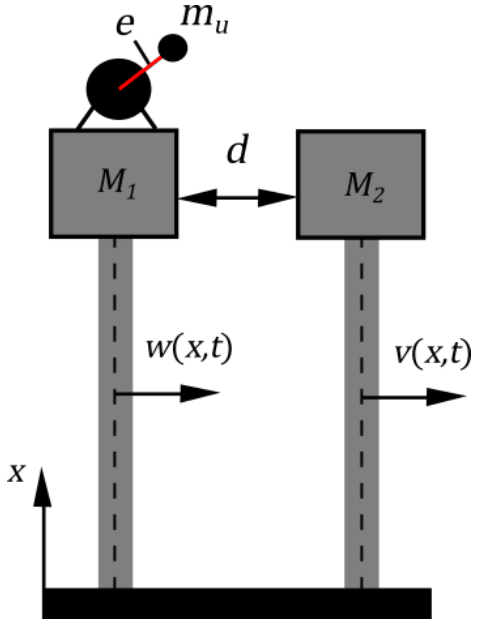

Figure 1: Schematic representation of the mechanical system studied.

where the subscripts $_{1,2}$ refer to each the beams, E is the Young's modulus, I is the area moment of inertia, ρ is the density, A is the cross-section area, $_c$ is the viscoelastic damping coefficient, δ_d is the Dirac delta function, ω is the excitation frequency or the motor rotating speed and F_c is the contact force. Three different contact force models were considered, which are presented in the following subsections. To obtain the responses of the beams, the modal expansion method was used, which considers the displacement of the beams to be the multiplication of two functions of only x and t, i.e.,

$$w(x,t)=\sum_{n=1}^{\infty}\phi_n(x)W_n(t) \tag{2.3}$$

$$v(x,t)=\sum_{n=1}^{\infty}\psi_n(x)V_n(x) \tag{2.4}$$

where $\phi_n(x)$ and $\psi_n(x)$ are the mass normalized eigenfunctions of the two beams, and $W_n(t)$ and $V_n(t)$ are the modal coordinates of the beams for the nth mode. The mass normalized eigenfunctions of the clamped-free beams are given by (Erturk and Inman, 2008);

$$\phi_n(x)=\sqrt{\frac{1}{\rho_1 A_1 L}}\left[\cosh\beta_n x-\cos\beta_n x-\left(\frac{\sinh\beta_n L-\sin\beta_n L}{\cosh\beta_n L+\cos\beta_n L}\right)\left(\sinh\beta_n x-\sin\beta_n x\right)\right] \tag{2.5}$$

$$\psi_n(x)=\sqrt{\frac{1}{\rho_2 A_2 L}}\left[\cosh\lambda_n x-\cos\lambda_n x-\left(\frac{\sinh\lambda_n L-\sin\lambda_n L}{\cosh\lambda_n L+\cos\lambda_n L}\right)\left(\sinh\lambda_n x-\sin\lambda_n x\right)\right] \tag{2.6}$$

where β_n and λ_n are the dimensionless natural frequencies of the nth mode of the beams and can be obtained through the characteristic equation, which for a clamped-free beam with tip mass is given as (Rao, 2007),

$$1+\frac{1}{\cos\alpha_n L\cosh\alpha_n L}-\frac{M_i}{\rho_i A_i L}\alpha_n L(\tan\alpha_n L-\tanh\alpha_n L)=0 \tag{2.7}$$

where α_n can be β_n or λ_n and $i=1,2$. The functions $\phi_n(x)$ and $\psi_n(x)$ satisfy the following orthogonality conditions,

$$\int_0^L \rho A f_r(x) f_n(x)dx=\delta_{rn},\quad \int_0^L EI f_r(x)\frac{d^4 f_n(x)}{dx^4}dx=\omega_n^2\delta_{rn} \tag{2.8}$$

where δ_{rn} is the Kronecker delta, which is zero for $r\neq n$ and one for $r=n$, ω_n is the undamped natural frequency of the nth mode of vibration, and f is an arbitrary function. By substituting Equations (2.3) and (2.4) into the equations of motion, Equations (2.1) and (2.2), and rearranging using the conditions of Equation (2.8), one has,

$$\ddot{W}_n(t)+2\zeta\omega_{n,1}\dot{W}_n(t)+\omega_{n,1}^2 W_n(t)=\phi_n(L)m_u e\omega^2\cos(\omega t)-\phi_n(L)F_c(t) \tag{2.9}$$

$$\ddot{V}_n(t)+2\zeta\omega_{n,2}\dot{V}_n(t)+\omega_{n,2}^2 V_n(t)=\psi_n(L)F_c(t) \tag{2.10}$$

where ζ is the damping factor, which is considered the same for both structures and for all of their modes of vibrations, $\omega_{n,i}$ is the undamped natural frequency of the beams and the dots represent a time differentiation. Equations (2.9) and (2.10) are linear and uncoupled ordinary differential equations when there is no contact, and nonlinear and coupled otherwise. After obtaining $W_n(t)$ and $V_n(t)$ the displacements of the beams at the free end are obtained from,

$$w(L,t)=\sum_{n=1}^{N}\phi_n(L)W_n(t) \tag{2.11}$$

$$v(L,t)=\sum_{n=1}^{N}\psi_n(L)V_n(t) \tag{2.12}$$

where N is the number of modes of vibration considered. In the simulations the number of modes was considered as $N=3$.

2.2 Hertz contact model

The Hertz contact model (GFF, 1896) was the first model developed to represent the interaction force at the surface of two contacting bodies (Gilardi and Sharf, 2002). However, the model was only valid when there was not much energy loss, as the damping was not included in the model. The Hertz contact model with nonlinear damping is given as (Hunt and Crossley, 1975),

$$F_c(t)=k_h\delta(t)^n+c_h\delta(t)^n\dot{\delta}(t)^p \tag{2.13}$$

where δ is the indentation or relative penetration, k_h is the impact stiffness which depends on the bodies mechanical properties, c_h is the impact damping coefficient which depends on the energy loss after the contact. For the contact of flat surfaces the exponents are commonly assumed as $n=1$ and $p=1$ (Gilardi and Sharf, 2002; Hunt and Crossley, 1975). The stiffness k_h for two isotropic spheres of radii R_1 and R_2, Poisson's ratios ν_1 and ν_2, and Young's modulus of E_1 and E_2, can be estimated by using (Goldsmith, 1960),

$$k_h=\frac{4}{3\pi}\left(\frac{1-\nu_1^2}{\pi E_1}+\frac{1-\nu_2^2}{\pi E_2}\right)^{-1}\left(\frac{R_1R_2}{R_1+R_2}\right)^{1/2} \tag{2.14}$$

for the impact of non-spheric objects, the equivalent sphere radius can be found using (Muthukumar and DesRoches, 2006),

$$R_{eq}=\left(\frac{3m}{4\pi\rho}\right)^{1/3} \tag{2.15}$$

where m is the mass of the object and ρ its density. In Lankarani and Nikravesh (1990), an equation for the impact damping coefficient (c_h) was proposed relating the coefficient of restitution and the impact stiffness, which has the form,

$$c_h=\frac{3k_h(1-e_1^2)}{4v_{rel}} \tag{2.16}$$

where e_1 is the coefficient of restitution, and v_{rel} is the magnitude of the relative approach velocity. The indentation for this model will be, $\delta=v(L,t)-w(L,t)-d$. Therefore, one can write the equation for the contact force, Equation (2.13), as,

$$F_c(t)=k_h[v(L,t)-w(L,t)-d]\left[1+\frac{3(1-e_1^2)}{4v_{rel}}\left(\frac{\partial v}{\partial t}(L,t)-\frac{\partial w}{\partial t}(L,t)\right)\right] \tag{2.17}$$

In the Hertz model, the contact force has always a positive value, thus when $F_c < 0$ or $\delta < 0$ it is assumed that $F_c = 0$, which means that the beams are not in contact. It is worth noting some qualitative aspects of the force model given by Equation (2.17):

- The damping force depends not only on the indentation rate of change but also on the indentation itself. This gives a more accurate model because the contact area increases as the indentation increases, which causes a plastic region to be developed when large deformations are reached;
- The contact force has no discontinuities at the beginning and at the end of the contact period, and, more importantly, the value of the force at these phases is zero. This feature has also been seen on experiments, showing the suitability of the model.

2.3 Viscoelastic Model

The viscoelastic or spring-dashpot model is one of the most widely used approaches for the study of impact (Howard and Kumar, 1993; Kraus and Kumar, 1997; Vukobratovic and Potkonjak, 1999; Mirza et al., 1993), mainly due to its simplicity and relatively good results. With the viscoelastic model the energy dissipation associated with the normal force is captured without considering plastic deformation issues (Gilardi and Sharf, 2002). The contact force according to the viscoelastic model is,

$$F_c(t) = k_v \delta(t) + c_v \dot{\delta}(t) \tag{2.18}$$

where k_v and c_v are the viscoelastic stiffness and damping coefficient, respectively. Despite the simplicity of implementing the viscoelastic contact force, it has three major disadvantages (Marhefka and Orin, 1999):

- The contact force given by Equation (2.18) is not continuous at the beginning and at the end due to the damping term. This gives non-zero values at these phases;
- At the end of the restitution phase, the velocity tends to a negative value and the indentation tends to zero. In the viscoelastic model this causes a tension force on the bodies at the separation point, which tends to hold them together;
- The coefficient of restitution defined based on this model is not dependent on the impact velocity. Several experiments have proven exactly the contrary, that the coefficient depends mostly on the velocity at the contact (Stoianovici and Hurmuzlu, 1996; Marghitu, 1997; Veluswami and Crossley, 1975; Nobre et al., 1999).

Using the indentation $\delta = v(L,t) - w(L,t) - d$, Equation (2.18) can be written as,

$$F_c(t) = k_v[v(L,t) - w(L,t) - d] + c_v\left[\frac{\partial v}{\partial t}(L,t) - \frac{\partial w}{\partial t}(L,t)\right] \tag{2.19}$$

When the bodies are in contact, the rate of change of the normal component of the relative velocity depends on the contact force and the indentation. Disregarding the damping force $c_v\dot{\delta}(t)$, the equation of the relative of the bodies is given as,

$$m_{ef}\ddot{\delta}(t) = -k_v\delta(t) \tag{2.20}$$

where $m_{ef}^{-1} = m_1^{-1} + m_2^{-1}$ is the effective mass, being m_1 and m_2 the masses of the bodies. Since $\ddot{\delta} = d\dot{\delta}/d\delta$, one can integrate Equation (2.20), which, using the initial conditions of $\delta(0) = 0$ and $\dot{\delta}(0) = -v_{rel}$, gives the following,

$$\dot{\delta}^2 = v_{rel}^2 - \frac{k_v}{m_{ef}}\delta^2 \tag{2.21}$$

the rate of change is zero at the end of the compression phase, and the indentation reaches a maximum value $\delta(t_c) = \delta_c$, where t_c is the time where the compression phase ends. Thus, the viscoelastic impact stiffness can be estimated by,

$$k_v = m_{ef}\left(\frac{v_{rel}}{\delta_c}\right)^2 \tag{2.22}$$

the parameters v_{rel} and δ_c must be found experimentally. According to Stronge (2004), the impact force obtained at the maximum indentation with the linear contact force gives a 14% less value than the one obtained with the Hertz theory. Since the impulse is the same, with a less force the viscoelastic model predicts a longer period of contact than the Hertz force. The viscoelastic impact damping was obtained using the following relation,

$$c_v = 2\zeta_v\sqrt{k_v m_{ef}} \tag{2.23}$$

being ζ_v the damping factor of the viscoelastic barrier.

2.4 Hard collision model

The first studies in the collision phenomenon were based in the assumption of rigid bodies. The premises of these models were a small contact area compared with the bodies cross-sectional areas and, most importantly, that the contact period is sufficiently small to be considered instantaneous. In the hard collision model the velocities after the impact are manually changed considering the coefficient of restitution (COR), which is a measure of the energy loss in the collision.

In the first hard collision model proposed by Sir Isaac Newton (1833) the COR was a kinematic quantity defined in terms of the normal velocities after and before the impact. After Newton, several other methods were proposed to obtain the COR, such as the Poisson's model (Wittenburg, 2013) which is defined as the ration between the impulses at the restitution and the compression phases, thus taking into account the kinetic of the collision. Also, Stronge (1991) proposed a COR model based on his internal energy dissipation hypothesis, which defines the COR as the square root of the ratio between the energy released during restitution and the energy absorbed during compression.

In this work, the Newton's COR model will be used. According to this model, the velocities of the bodies after the impact can be written as (Muthukumar and DesRoches, 2006),

$$\begin{aligned} v_1' &= v_1 - (1+e_1)\frac{m_2(v_1 - v_2)}{m_1 + m_2} \\ v_2' &= v_2 + (1+e_1)\frac{m_1(v_1 - v_2)}{m_1 + m_2} \end{aligned} \tag{2.24}$$

where v_1' and v_2' are the bodies' velocities after the impact, v_1 and v_2 are the velocities before the impact and m_1 and m_2 are the bodies' masses. To implement the hard collision model, the equations of motion, Equations (2.9) and (2.10) with $F_c = 0$, were solved using the Runge-kutta scheme, and if the condition $\delta \geq 0$ was satisfied, the velocities of the bodies were changed using Equations (2.24). Also, the coefficient of restitution, e_1, used was the same for Equations (2.24) and (2.16).

3 EXPERIMENTAL SETUP

The experiments were carried out at the Intelligent Materials and Control Laboratory in the Ilha Solteira Campus of the São Paulo State University (UNESP). The signals were obtained using a sample frequency of 2048 Hz and a time of measurement of 14 s. The experimental setup consist in two identical portal frame structures positioned side by side by a distance of 1 mm, being one of the structures excited by an unbalanced DC motor as shown in Figure 2. The columns of the shear-building structures were manufactured using ASTM A-36 steel with dimensions 1.75 mm×76.2 mm×300 mm, which correspond to the thickness, width and length, respectively. The floor and the top of the structures are made from polypropylene plates with dimensions of 15 mm×76.2 mm×400 mm. In addition, Allen

bolts were used to connect the columns with the floor and top. The impacting surfaces were the heads of the Allen bolts, which were sandpapered to reduce the influence of friction in the responses.

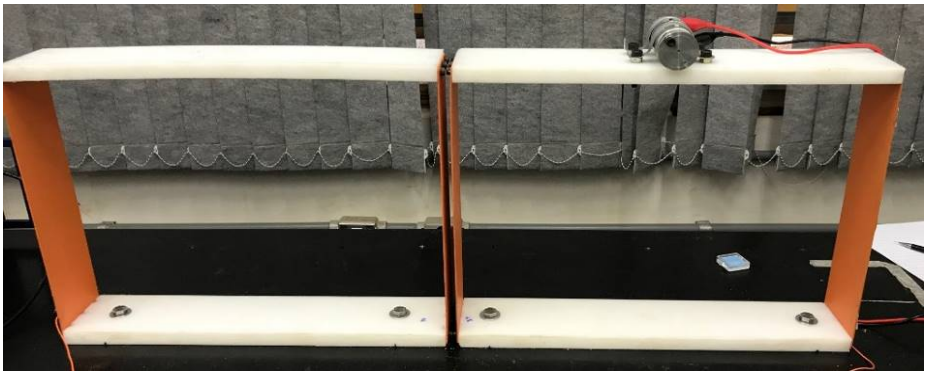

Figure 2: Mechanical system studied: two identical portal frame structures.

(a) (b)

Figure 3: Location of the Accelerometers: (a) Structure with the motor and (b) structure without the motor.

Table 1: Properties of the DC motor used.

Property	Value
Nominal Voltage	24 V
Stall Current	2.5 A
Stall Torque	28.7 Ncm
No Load Speed	4550 rpm
Start Up Voltage	2 V
Weight	224 g
Shaft Diameter	3.1 mm
Shaft Length	85 mm
Motor Diameter	37 mm
Motor Length	64 mm

The DC motor used was a Mabuchi DC motor model C2162-60006 powered by a power source of Minipa model MPL-3303M, and it was mounted in the middle of the top of the excited structure as shown in Figure 2. Table 1 shows more information about the motor used. The motor was unbalanced by placing a mass of 6.59 g in a distance of 15 mm from the axis of rotation. In addition, the structures were bolted in an inertial bench to prevent vibrations from other sources to interfere in the measurements.

In order to measure the accelerations of the structures, two accelerometers were positioned at the top of the no impacting column of each structure as shown in Figure 3. The accelerometers used were from Dytran Instruments Inc. model 2335F1, which have sensitivity of 9.89 mV/g. For the acquisition and data analysis a LMS Scadas Mobile model VB8-II from Siemens was used.

4 IMPACT AND DAMPING PARAMETERS

In this section the main impact parameters as well as the damping factor of the model will be obtained based on the mechanical system presented in the previous section. From now on, the shear-building with the DC motor will be referred as structure 1 and the other shear-building as structure 2.

First, the impact parameters corresponding the the Hertz model are obtained. Initially, the equivalent sphere radius of the structures are obtained using Equation (2.14), which gave $R_1 = 30.7$ and $R_2 = 28.1$ mm for structure 1 and 2, respectively. As both structures are made from the same materials, their mechanical properties are the same, $E_1 = E_2 = 200$ GPa and $\nu_1 = \nu_2 = 0.33$. From these values, the impact stiffness is obtained using Equation (2.13),

$k_h = 2.31 \times 10^{10}$ N/m$^{3/2}$

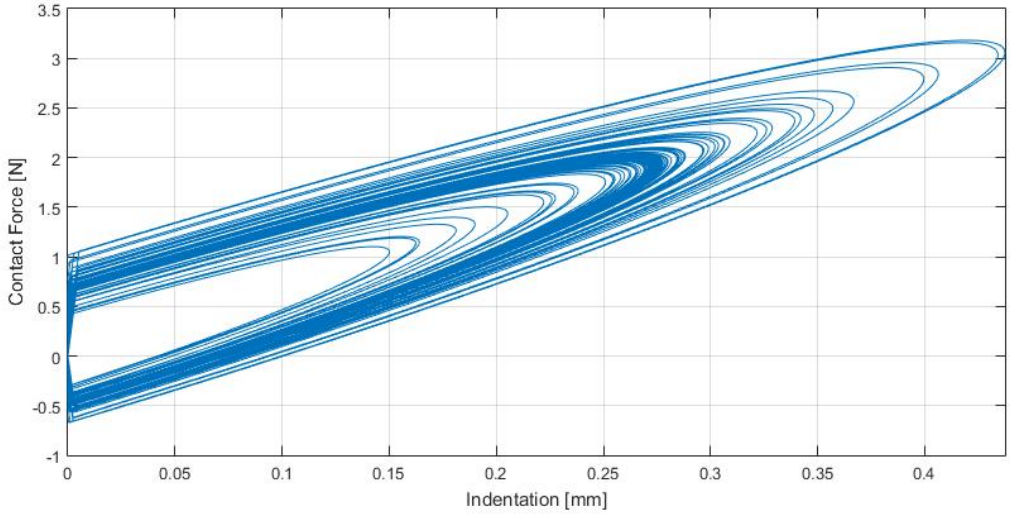

Figure 4: Viscoelastic contact force vs indentation with a high damping coefficient c_v.

In order to obtain the impact damping parameter, c_h, the coefficient of restitution, e_1, and the relative approach velocity, v_{rel} have to be obtained experimentally. The procedure followed to obtain these parameters was to integrate the acceleration signals measured and to take the velocities after and before the impacts in the whole time of measurement, and then taking the mean values. This procedure gave the values for the coefficient of restitution and the approach velocity as $e_1 = 0.8$ and $v_{rel} = 0.1644$ m/s. With these parameters at hand, the impact damping was obtained using Equation (2.15),

$c_h = 1.01 \times 10^{11}$ Ns/m$^{5/2}$

Now obtaining the parameter corresponding to the impact stiffness in the viscoelastic model, k_v, Equation (2.21) is used, giving a value of,

$k_v = 6.99 \times 10^{6}$ N/m

In obtaining k_v, as the maximum indentation δ_c could not be obtained by the measurements performed, it was assumed that $\delta_c = 4 \times 10^{-5}$ m. Furthermore, to obtain the damping parameter c_v, the viscoelastic damping factor ζ_v was

varied so that the effect of the negative value of the viscoelastic force at the end of the restitution phase could be minimized. Figure 4 shows the contact force vs indentation graph for several loadings due to dynamic forces in a case where the damping coefficient c_v is high. As one can

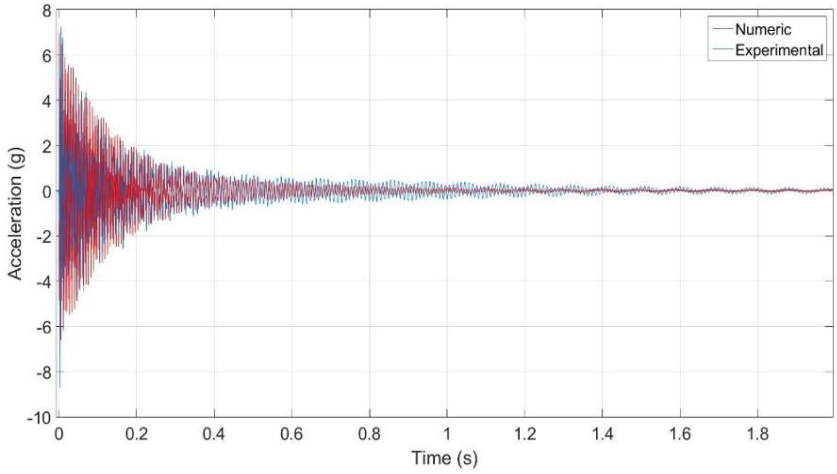

Figure 5: Comparison between the experimental and the numeric signals for the free vibration of structure 2.

note from the figure, the contact force gets negative in a wide range of indentation values during the loadings generated by the impacts, which influence the velocity after the successive impacts. Thus, to minimize this effect, the damping factor was assumed as $\zeta_v = 0.05$, and, using Equation (2.22), the following damping coefficient was obtained,

$$c_v = 170.07 \text{ Ns/m}$$

In addition, the damping factor was assumed the same for both structures and it was obtained by measuring the free vibration of both structures and taking the peaks values of the signals. The damping factor obtained was $\zeta = 0.003$. In addition, Figure 5 presents the comparison between the experimental signal and the numeric one for structure 2. As one can note by the figure, the numeric response was very close to the experimental data.

5 RESULTS AND DISCUSSION

The system was analyzed in four different rotational speeds of the unbalanced motor, which corresponded to the regions of resonance, pre-resonance, post-resonance and a case with no excitation of the motor. The resonance frequency is related to the first natural frequency of structure 1. In the case with no excitation frequency, an initial displacement was given to structure 1 sufficient for the contact to occur. In each of the cases analyzed the acceleration of both structures were measured using accelerometers.

For the continuous models, Hertz and Viscoelastic models, the sample frequency used in the simulations was 4096 Hz, and the Adams-Bashforth-Moulton integration scheme was used in the solution of the equations. These high sample frequency and integration scheme are used because the system is stiff. In the case of the hard collision model, the equations were solved by the Runge-Kutta scheme and the sample frequency was 1500 Hz. This latter case presented the results much faster than the continuous models. The models were simulated up to 100 s in order to avoid the influence of the transient part in the response of the system.

In the next subsections, the results of each case analyzed are shown with the comparison with the vibro-impact models discussed. To validate the models, two characteristics presented by them were compared with the measured signals: the amplitude of the acceleration and the impact per oscillation. The latter gives a qualitative idea of the model and shows how suitable it is to the measured signal and it is also useful in designing systems to control the impacts. As for the acceleration amplitude, it gives a quantitative idea, which is very important in the design of the structures and the determination of the critical stresses that they are subjected.

The models were also analyzed in the frequency domain by means of the Continuous Wavelet Transform (CWT) and the Persistence Spectrum based on the Power Spectrum Density. The Wavelet transform is an important mathematical tool to analyze nonlinear systems and signals in the non-stationary regime. Some examples of the application of the

wavelet transform in nonlinear systems are presented in Varanis et al. (2018a,c); Piccirillo et al. (2016). In addition, in the analysis made with the wavelet transform, the Mayer filter was used.

5.1 Resonance region

Figure 6 presents the accelerations of Structure 1 in the case when the excitation frequency matched the first natural frequency of Structure 1, where the peaks represent the accelerations due to contact. The figure presents the accelerations obtained by the three models presented before and the experimental signal for Structure 1. The acceleration signal of Structure 2 presented the same characteristics as the signal shown in Figure 6b, except for higher acceleration peaks.

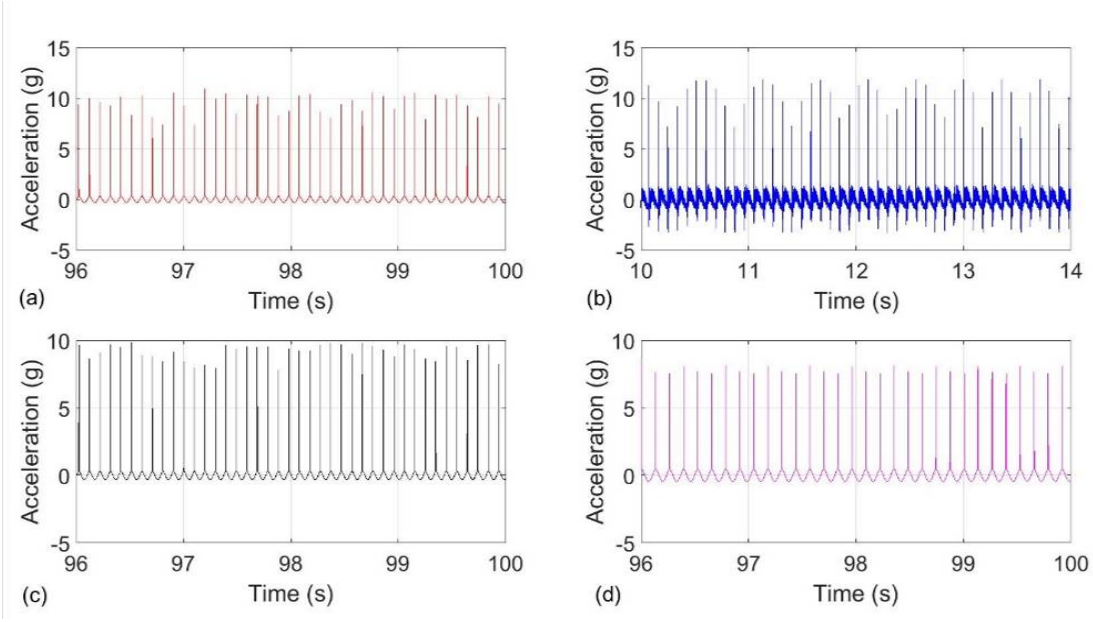

Figure 6: Comparison between the experimental and the numeric signals for the excitation frequency at the resonance for Structure 1: (a) Hertz model, (b) Experimental signal, (c) Viscoelastic model and (d) Hard collision model.

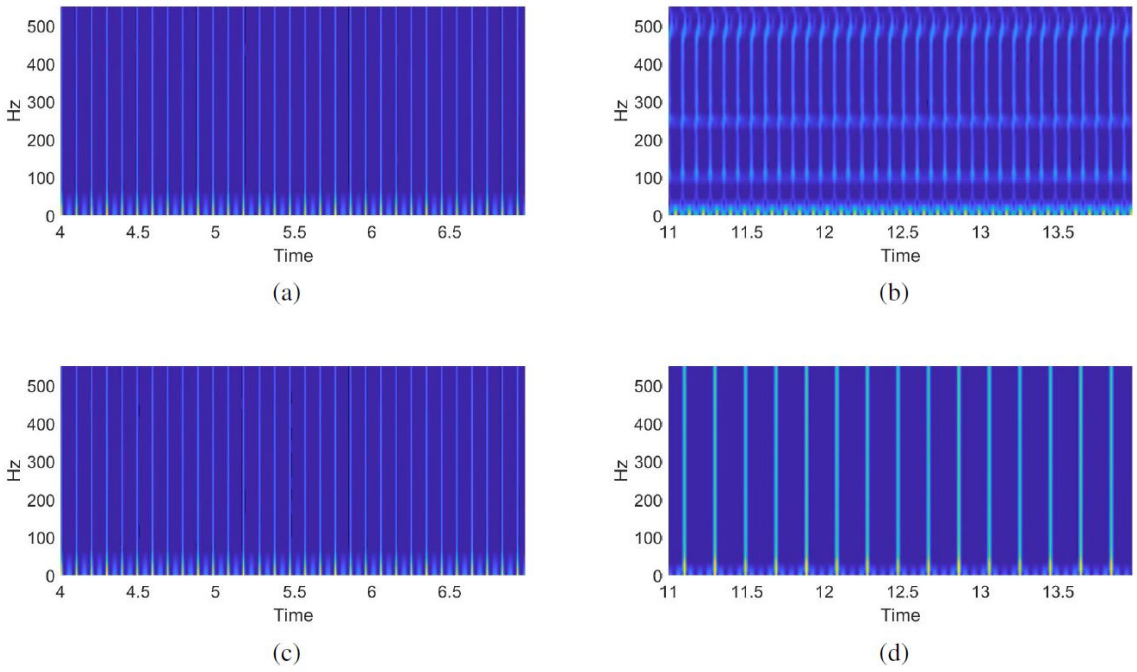

Figure 7: CWT of the signals at resonance: (a) Hertz model, (b) Experimental signal, (c) Viscoelastic model and (d) Hard collision model.

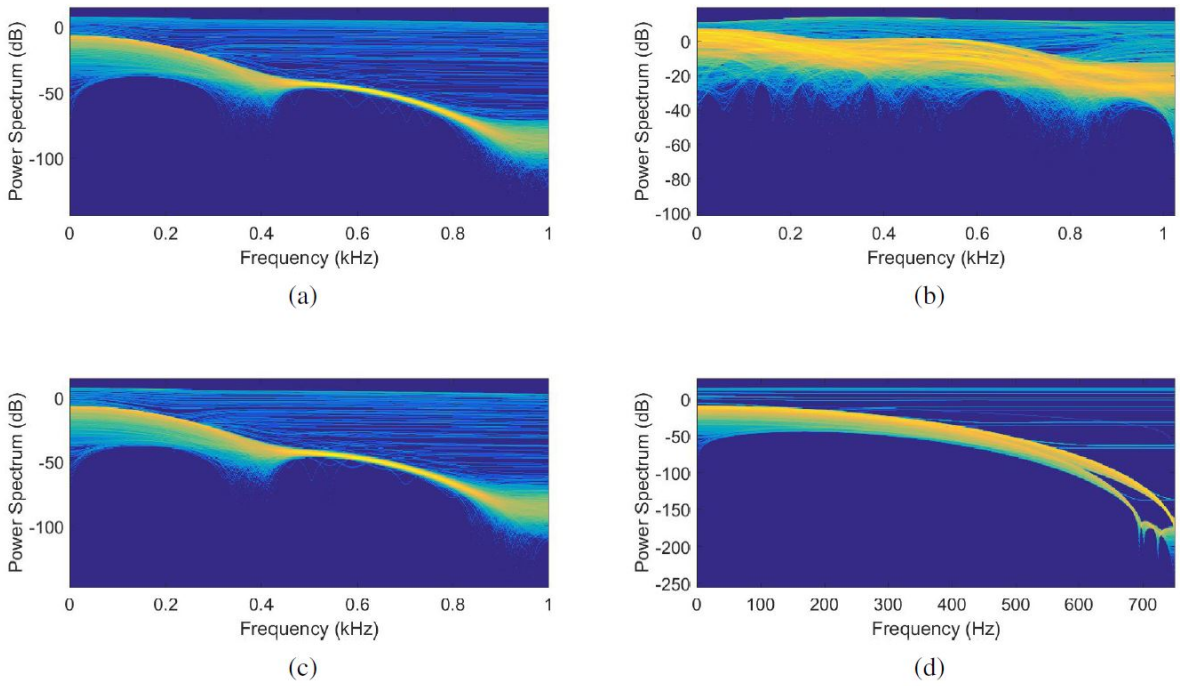

Figure 8: Persistence Spectrum of the signals at resonance: (a) Hertz model, (b) Experimental signal, (c) Viscoelastic model and (d) Hard collision model.

As it can be expected, this was the case with the most intense contact, since the amplitude of the structures were high. By comparing the numeric signals, Figures 6a, 6c and 6d, with the experimental signal, Figure 6b, it is seen that the models presented good agreement with the measurements. The maximum acceleration measured in the Structure 1 was around 11.95 g, and the values given by the Hertz, Viscoelastic and Hard Collision models were 10.9 g, 9.8 g, and 8.1 g, respectively. The model with presented more deviation from the experimental signal was the Hard Collision model, although this model is much easier to implement numerically. These values show that the models can be used with considerable accuracy at the resonance region when the maximum accelerations due to contact need to be obtained.

In addition, by comparing the features given by the models with the experimental signal in Figure 6, it is noted that in the experimental signal the impact forces varies its intensity due to the out-of-phase movement of the structures and there is an influence in the higher modes of vibration in the dynamic response of the structure. By looking at the numeric signals in Figure 6, one can note that the three models presented such characteristics, which shows that they represent very accurately the experimental signal. It is worth noting that the higher modes of vibration in the models did not affect the outcome, because the amplitudes in the second and third modes could not surpass the gap imposed $d = 1$ mm.

Figures 7 and 8 present the Continuous Wavelet Transform and the Persistence Spectrum of the signals of Figure 6. It can be seen that the frequency spectrum of the experimental signal (Figure 7b) presented similar responses when compared with the numerical signals, where a localization of power in time and frequency is obtained. The analysis by the Persistence spectrum, Figure 8, shows that the distribution of the frequencies of the numeric signals were similar to the experimental signals.

5.2 Post-resonance region

In the other case studied, presented in Figure 9, the excitation frequency was slightly higher than the natural frequency, specifically 17% higher, so that the beating phenomenon could be seen. In this case the models predicted peak accelerations that were slightly different to the measured values, as it can be noted comparing the experimental signal, Figure 9b, with the numeric signals given by the models, Figures 9a, 9c and 9d. While the peak acceleration measured was around 5.17 g, the Hertz and Viscoelastic models predicted accelerations around 8 g and the Hard collision a value around 16 g.

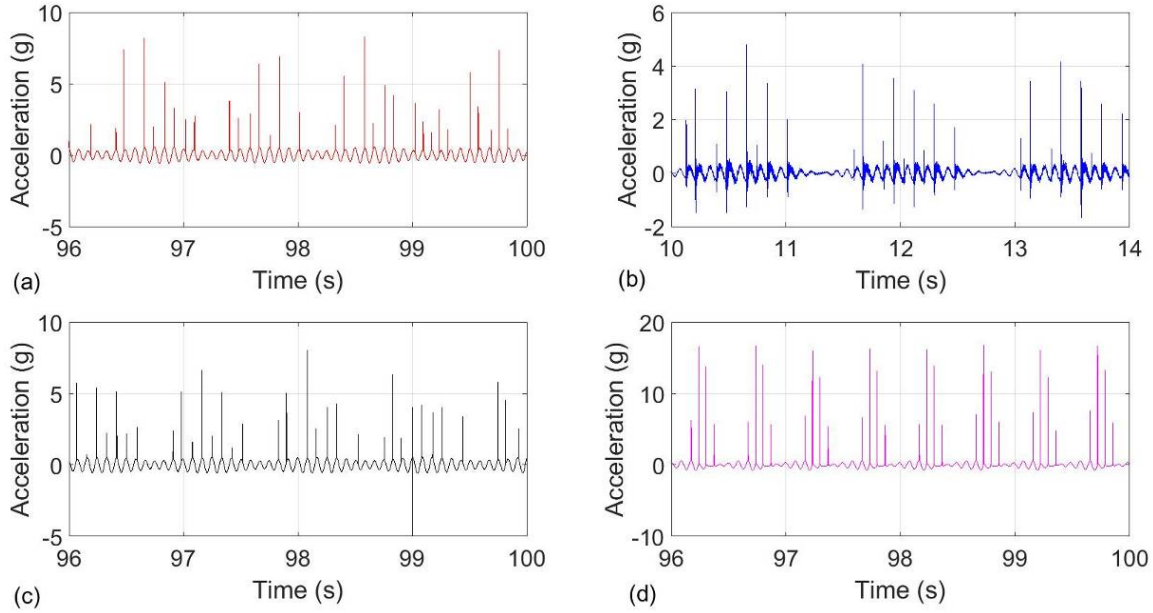

Figure 9: Comparison between the experimental and the numeric signals for the excitation frequency at the post-resonance for Structure 1: (a) Hertz model, (b) Experimental signal, (c) Viscoelastic model and (d) Hard collision model.

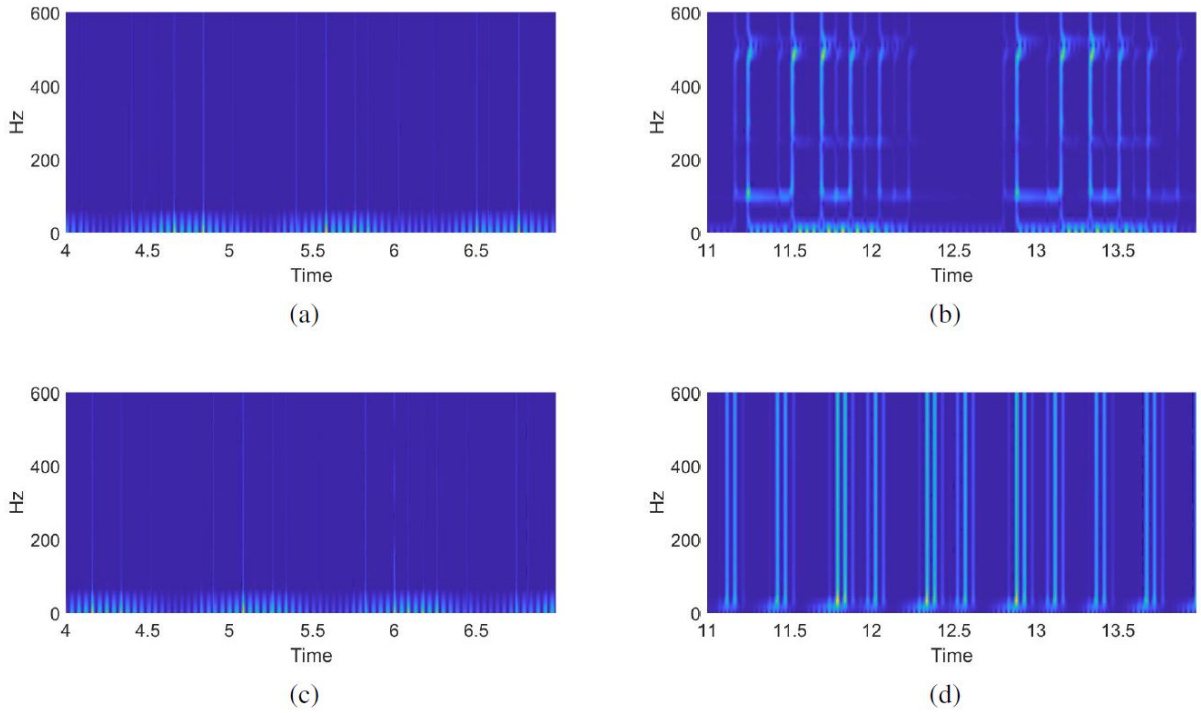

Figure 10: CWT of the signals at post-resonance: (a) Hertz model, (b) Experimental signal, (c) Viscoelastic model and (d) Hard collision model.

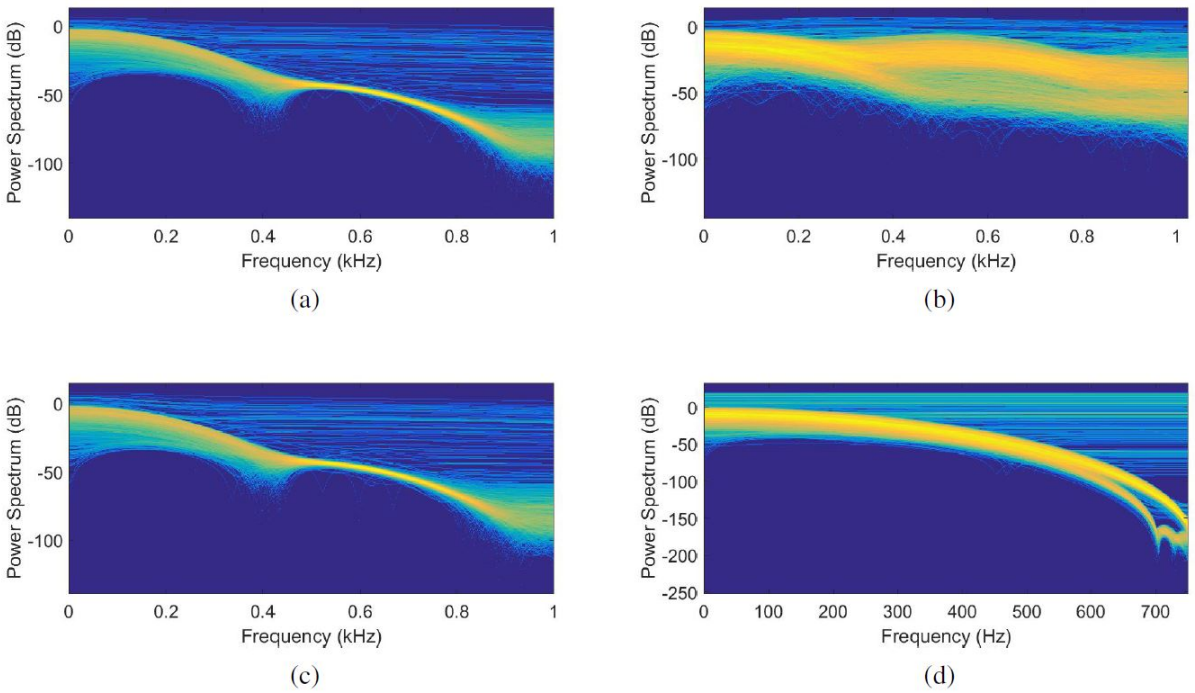

Figure 11: Persistence Spectrum of the signals at post-resonance: (a) Hertz model, (b) Experimental signal, (c) Viscoelastic model and (d) Hard collision model.

By analyzing the figure in a qualitative point of view, one may note that the models, despite showing very different acceleration values, showed a good agreement with the experimental signal, being the impacts per oscillations closely related. If the oscillation due to the beating frequency is taken into account, the experimental signal presented around 8 impacts per beating oscillation, while the Hertz, Viscoelastic and Hard collision models presented around 8, 7 and 4, respectively. It is worth noting that these values were not the same for the whole time series. This qualitative agreement of the models with the experiments can be beneficial in designing a controller for the real structure or predicting a no impacting region. Between the models, the Hertz model, Figure 9a, presented more suitability with the experimental signal, Figure 9b, since the impacts per unit of oscillation were very close. As it can be noted in Figure 9, there is a strong influence in the higher modes of vibration in the behavior of the structure. However, similarly as the responses in the resonance case, the higher modes of vibration did not influence much the simulations, since the amplitude of structure 1 was not enough to surpass the gap distance in the second and third modes of vibration. The effect of the higher modes in the model can be taken into account by considering a nonlinear equation with coupled modes of vibration, which was not performed in this work.

The analysis in the frequency domain, Figures 10 and 11, showed that the models represented well the experimental signal. The CWT of the Hertz and Viscoelastic models were very similar, and the Hard collision presented a wide frequency excitation due to impacts, as it can be noted by the Persistence Spectrum in Figure 10d. The Persistence Spectrum, Figure 11, showed once more that the frequency distribution of the numeric signals were close to the experimental.

5.3 Pre-resonance region

In the case where the system was in the region of pre-resonance, presented in Figure 12, the excitation frequency was 95% the first natural frequency of Structure 1. In this case the system presented a weak beating characteristic. As it can be seen comparing the numeric signals, Figures 12a, 12c and 12d, with the experimental signal, Figure 12b, the maximum accelerations predicted were not in agreement with the values measured, but they were closer than the difference seen in the post-resonance case. While the experimental value was around 5.14 g, the Hertz, Vicoelastic and Hard Collision models predicted values of 11.3 g, 12.05 g and 6.6 g. The best result was the one presented by the Hard Collision model with an error of 28% comparing with the measured one, which, depending on the application, shows that the model can be used with considerable accuracy.

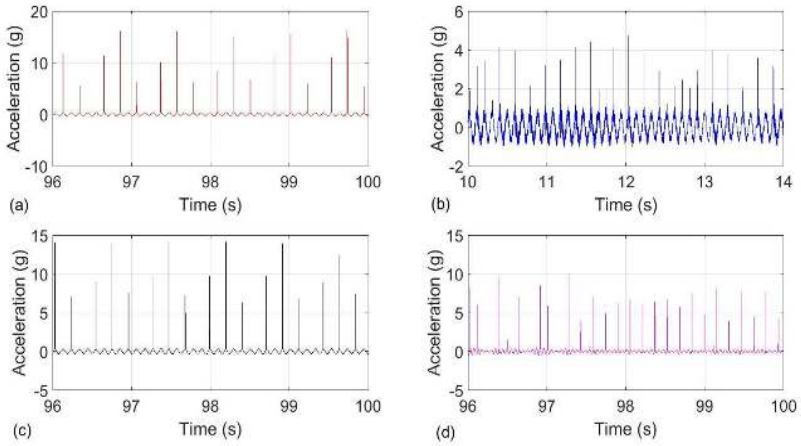

Figure 12: Comparison between the experimental and the numeric signals for the excitation frequency at the pre-resonance for Structure 1: (a) Hertz model, (b) Experimental signal, (c) Viscoelastic model and (d) Hard collision model.

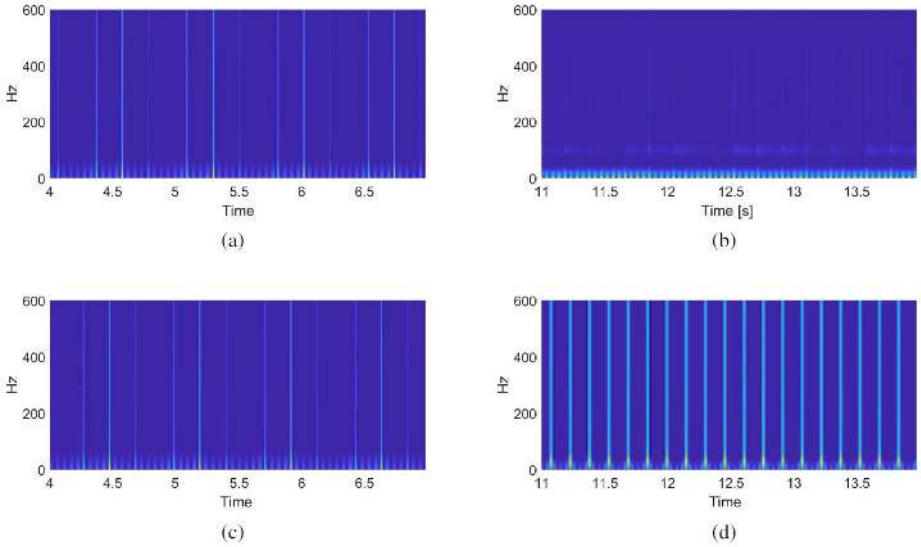

Figure 13: CWT of the signals at pre-resonance: (a) Hertz model, (b) Experimental signal, (c) Viscoelastic model and (d) Hard collision model.

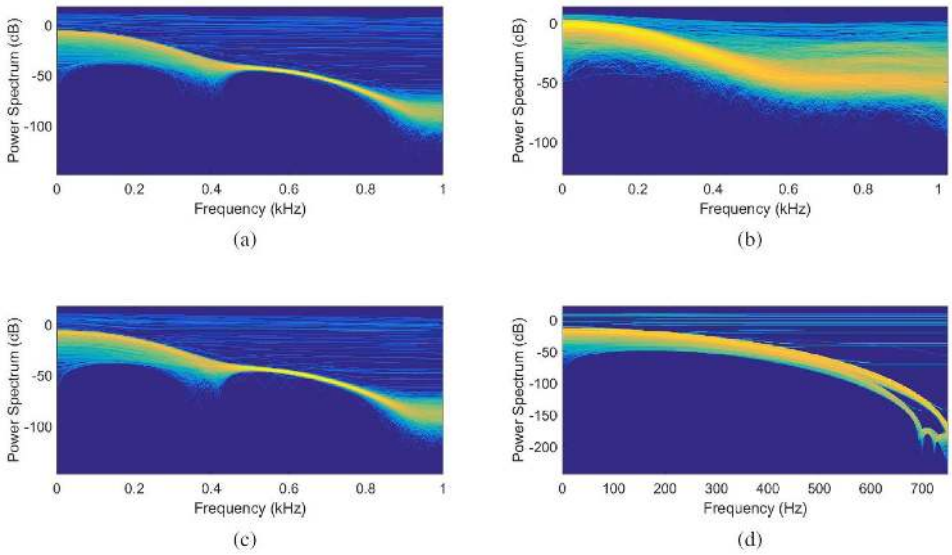

Figure 14: Persistence Spectrum of the signals at pre-resonance: (a) Hertz model, (b) Experimental signal, (c) Viscoelastic model and (d) Hard collision model.

A closer look in the results for a qualitative analysis, it can be seen that the models presented a considerable qualitative agreement with the experimental signal, as the impact per oscillation predicted by them were very close with the measured ones. In this case, the Hertz and Vicoelastic models showed very similar characteristics, and the Hard Collision, despite giving the closer peak acceleration, showed a different number of impacts per oscillation comparing with the experimental signal. The results also show that the dynamic behavior of the contact force, which can be noted by the peaks in Figure 12, was captured by the models.

The analysis in the frequency domain is presented in Figures 13 and 14. The Figures show that the models presented similar characteristics in the frequency domain when compared with the experimental signal. This case was the least energetic case as one can note from the CWT of the experimental signal (Figure 13). On the other hand, the models predicted impacts with more intensity, specially the Hard collision model. The distribution of the frequency spectrum of the numeric and experimental signal were, however, very close as shown by the Persistence Spectrum in Figure 14.

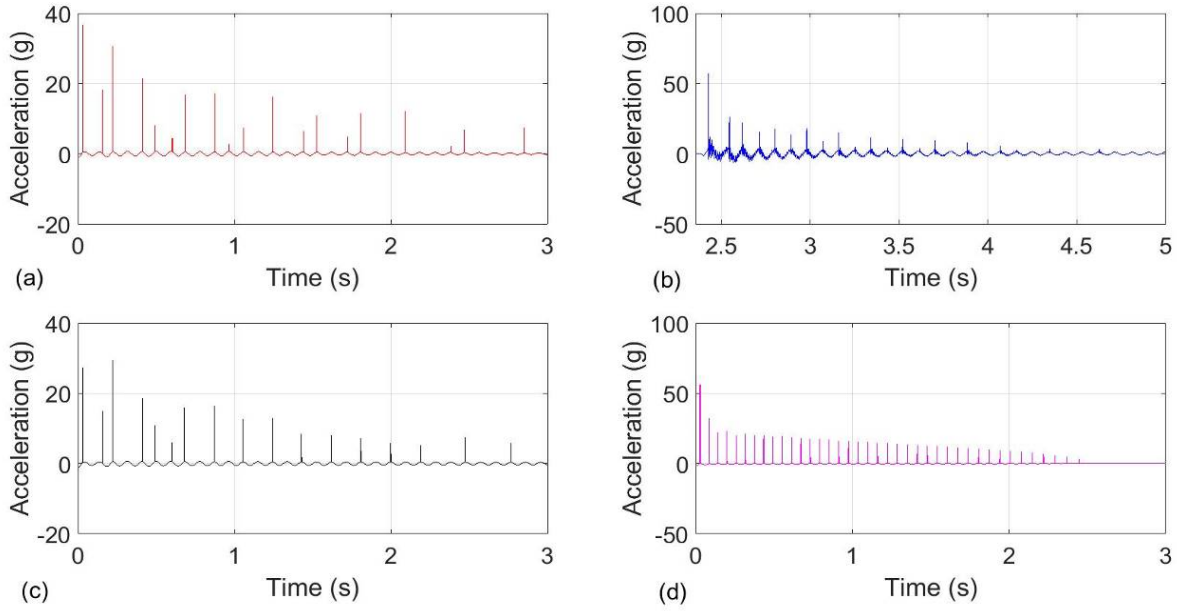

Figure 15: Comparison between the experimental and the numeric signals for the case with an initial condition: (a) Hertz model, (b) Experimental signal, (c) Viscoelastic model and (d) Hard collision model.

5.4 Free vibration

In the last case studied, the system was analyzed in a non-stationary situation, where the unbalanced motor in Structure 1 was turned off and an initial displacement condition was given to it to obtain the measurements. Figure 15 shows the results of the simulations and the experimental signal measured. By comparing the responses of the models, Figure 15a, 15c and 15d, with the experimental signal 15b, it is noted that the simulations were in according with the measurements. The model that presented the best results was the Hard Collision model, which showed peak accelerations that were very close with the experimental values. The Viscoelastic model presented good results as well when compared with the experimental signal, and the worse result was obtained with the Hertz model. In a qualitative point of view, all the three models presented good results showing that they can be used in non-stationary analysis as well, with considerable accuracy. This analysis can be very useful in situations where two adjacent structures are given initial conditions, in such cases, the models presented here can be used to study the accelerations and impacts per oscillations.

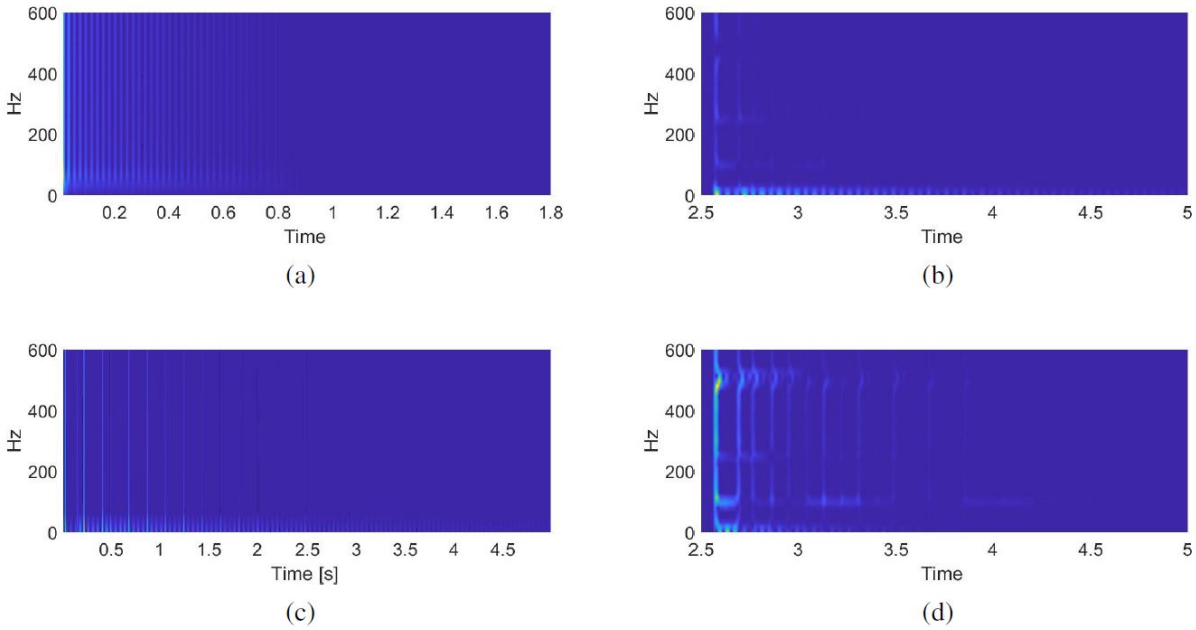

Figure 16: CWT of the signals for the free vibration case: (a) Hertz model, (b) Experimental signal, (c) Viscoelastic model and (d) Hard collision model.

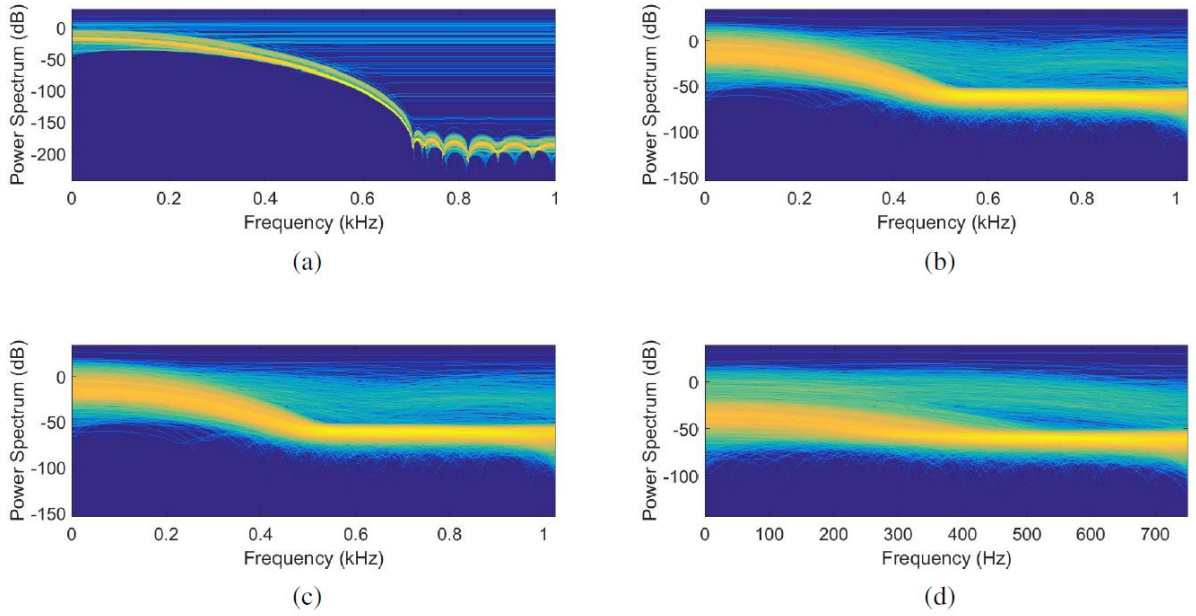

Figure 17: Persistence Spectrum of the signals for the free vibration case: (a) Hertz model, (b) Experimental signal, (c) Viscoelastic model and (d) Hard collision model.

The frequency analysis in the free vibration showed in Figures 16 and 17. Figure 16 shows that the content of the frequency spectrum of the experimental signal is very similar to that of the numeric ones. The Hard collision model showed the best results. The Persistence Spectrum of the signals, Figure 17, show that the frequency distribution of the experimental signal was very similar to the numeric ones.

6 CONCLUSIONS

This paper presented a continuous vibration model for two shear-building structures subjected to impacts, being one of the structures driven by an unbalance DC motor. The impacts were modeled by means of three different models: the Hertz model, the Viscoelastic model and the Hard Collision model. The first two models consist in continuous models where a force-deflection relation must be given to predict the deformation of the impacting bodies. In the Hard Collision

model, however, the bodies are considered rigid and the time of contact instantaneous. Since in this case the equations are simple, the numerical simulations were faster when compared to the other two models. In addition, the Hard Collision model showed to be more appropriate for the mechanical system studied, since the time of contact between the structures was very small. This led the numerical simulations of the Hertz and Viscoelastic models to be very stiff, which in turn made the simulations very time consuming.

In order to validate the models, experimental measurements were performed and the signals obtained compared with the responses given by the models. The structures were analyzed in four different cases: in the resonance region, in the post-resonance, in the pre-resonance, and in a non-stationary case, where an initial displacement was given to one of the structures. In all the cases the accelerations of the structures were measured using accelerometers. In the first situation studied, when the excitation frequency of the motor matched the natural frequency of Structure 1, the simulations showed good qualitative and quantitative agreement with the experimental signal. In this case, the model that predicted the peak accelerations that were closer with the measured values was the Hertz model.

In the other excitation frequencies considered, which corresponded to the regions of post- and pre-resonance, the simulations did not predict the peak accelerations measured, but the models represented well the mechanical system in a qualitative view. The worse predictions presented by the models was in the post-resonance region, where the peak accelerations were very different from the values measured. However, as discussed, a qualitative analysis showed that the models, despite giving very different quantitative values, were in agreement in a qualitative point of view, as they presented a close impact per oscillation number with the experimental value. Thus the models can be used for the study of the dynamics of the system and for the designing of a controller for the impacts. In the last case studied, the system was analyzed in a non-stationary situation, where an initial displacement was given to structure 1 enough for the impact to occur. The simulations showed results that were in agreement with the experimental signal measured, showing that the models can be used to analyze the mechanical system with considerable accuracy.

The analysis performed in the frequency domain using the Continuous Wavelet Transform and the Persistence spectrum showed that the responses of the models presented similar spectral contents as the experimental signal. The best results regarding the frequency characteristics of the signals were given by the Hard collision model. In addition, the Persistence Spectrum showed that the frequency distribution of the numeric signals were in accordance with the experimental ones.

It is important to point out that the higher modes of vibration considered in the models did not influence the responses because the displacement in that modes were much smaller than the gap distance between the structures, thus leaving the second and third modes unaffected by the impacts. On the other hand, the experimental signals presented an influence of the higher modes in the behavior of the system. One way to account these modes in the response of the models is considering a nonlinear model with coupled modes of vibration, thus the impacts occurring in the first mode would influence the higher modes of vibration.

References

Aguiar, R. and Weber, H., 2012. “Impact force magnitude analysis of an impact pendulum suspended in a vibrating structure”. *Shock and Vibration*, Vol. 19, No. 6, pp. 1359–1372.

Aoki, S. and Watanabe, T., 1997. “Stationary random vibration of mechanical system with collision characteristics”. In *Vibration Conference*. Vol. 1, pp. 185–190.

Brach, R.M., 1998. “Formulation of rigid body impact problems using generalized coefficients”. *International journal of engineering science*, Vol. 36, No. 1, pp. 61–71.

Choy, F., Padovan, J. and Li, W., 1988. “Rub in high performance turbomachinery, modeling, solution methodology and signature analysis”. *Mechanical Systems and Signal Processing*, Vol. 2, No. 2, pp. 113–133.

Dubowsky, S. and Freudenstein, F., 1971. “Dynamic analysis of mechanical systems with clearancesâA Tpart 1: formation of dynamic model”. *Journal of Engineering for industry*, Vol. 93, No. 1, pp. 305–309.

Erturk, A. and Inman, D.J., 2008. “On mechanical modeling of cantilevered piezoelectric vibration energy harvesters”. *Journal of Intelligent Material Systems and Structures*, Vol. 19, No. 11, pp. 1311–1325.

GFF, G., 1896. “Hertz’s miscellaneous papers”. *Nature*, Vol. 55, pp. 6–9.

Gilardi, G. and Sharf, I., 2002. “Literature survey of contact dynamics modelling”. *Mechanism and machine theory*, Vol. 37, No. 10, pp. 1213–1239.

Goldsmith, W., 1960. “Impact: the theory and physical behaviour of colliding solids”. Edward Arnold, London.

Hiwarkar, V.R., Babitsky, V.I. and Silberschmidt, V.V., 2011. “Vibro-impact response of a cracked bar”. *Shock and Vibration*, Vol. 18, No. 1, 2, pp. 147–156.

Howard, W.S. and Kumar, V., 1993. “A minimum principle for the dynamic analysis of systems with frictional contacts”. In *Robotics and Automation, 1993. Proceedings., 1993 IEEE International Conference on*. IEEE, pp. 437–442.

Hunt, K. and Crossley, F., 1975. “Coefficient of restitution interpreted as damping in vibroimpact”. *Journal of applied mechanics*, Vol. 42, No. 2, pp. 440–445.

Ibrahim, R.A., 2009. *Vibro-impact dynamics: modeling, mapping and applications*, Vol. 43. Springer Science & Business Media.

Kobrinskij, A., 1964. “Mechanisms with elastic constraints”.

Kraus, P.R. and Kumar, V., 1997. “Compliant contact models for rigid body collisions”. In *Robotics and Automation, 1997. Proceedings., 1997 IEEE International Conference on*. IEEE, Vol. 2, pp. 1382–1387.

Lankarani, H. and Nikravesh, P., 1990. “A contact force model with hysteresis damping for impact analysis of multibody systems”. *Journal of mechanical design*, Vol. 112, No. 3, pp. 369–376.

Lok, H. and Wiercigroch, M., 1996. “Modelling discontinuities in mechanical systems by smooth functions”. In *EUROMECH-Second European Nonlinear Oscillations Conference, Prague*. pp. 121–176.

Marghitu, D., 1997. “The impact of flexible links with solid lubrication”.

Marhefka, D.W. and Orin, D.E., 1999. “A compliant contact model with nonlinear damping for simulation of robotic systems”. *IEEE Transactions on Systems, Man, and Cybernetics-Part A: Systems and Humans*, Vol. 29, No. 6, pp. 566–572.

Mereles, A., Varanis, M., Balthazar, J. and Tusset, A., 2018. “Seismic pounding model using hertzian contact”. In *X Congresso Nacional de Engenharia Mecâcnica*. ABCM.

Mereles, A., Varanis, M., Balthazar, J., Tusset, A., Rocha, R. and Oliveira, C., 2017a. “Evaluation of a cantilever beam energy harvester subjected to impacts”. In *XXXVIII Iberian-Latin American Congress on Computational Methods in Engineering*. ABMEC.

Mereles, A., Varanis, M., Silva, A., Balthazar, J. and Pederiva, R., 2017b. “Evaluation of impact models for body-tobarrier collisions”. In *Procceedings of the 24th ABCM International Congress of Mechanical Engineering, 2017*. ABCM.

Mirza, K., Hanes, M.D. and Orin, D.E., 1993. “Dynamic simulation of enveloping power grasps”. In *Robotics and Automation, 1993. Proceedings., 1993 IEEE International Conference on*. IEEE, pp. 430–435.

Moraes, F.H., Pontes Jr, B.R., Silveira, M., Balthazar, J.M. and Brasil, R.M., 2013. “Influence of ideal and non-ideal excitation sources on the dynamics of a nonlinear vibro-impact system”. *Journal of Theoretical and Applied Mechanics*, Vol. 51, No. 3, pp. 763–774.

Muthukumar, S. and DesRoches, R., 2006. “A hertz contact model with non-linear damping for pounding simulation”. *Earthquake engineering & structural dynamics*, Vol. 35, No. 7, pp. 811–828.

Navarro, H.A., Balthazar, J.M. and Brasil, R.M., 2014. “Vibrations due to impact in a non ideal mechanical system with a non-linear hertzian contact model”. In *ASME 2014 International Design Engineering Technical Conferences and Computers and Information in Engineering Conference*. American Society of Mechanical Engineers, pp. V008T11A041–V008T11A041.

Newton, I., 1833. *Philosophiae naturalis principia mathematica*, Vol. 1. G. Brookman.

Nobre, J., Dias, A. and Gras, R., 1999. “A study on elasto-plastic impact friction”. *Wear*, Vol. 230, No. 2, pp. 133–145.

Papadrakakis, M., Mouzakis, H., Plevris, N. and Bitzarakis, S., 1991. “A lagrange multiplier solution method for pounding of buildings during earthquakes”. *Earthquake engineering & structural dynamics*, Vol. 20, No. 11, pp. 981–998.

Peterka, F., 1981. “Introduction to vibration of mechanical systems with internal impacts”. *Prague: Academia*.

Peterka, F. and Tondl, A., 2004. “Phenomena of subharmonic motions of oscillator with soft impacts”. *Chaos, Solitons & Fractals*, Vol. 19, No. 5, pp. 1283–1290.

Pfeiffer, F., 1987. “On unsteady dynamics in machines with plays”. In *Proc. 7th World Congress on TMM*. Vol. 1, pp. 471–423.

Piccirillo, V., Balthazar, J.M., Tusset, A.M., Bernardini, D. and Rega, G., 2016. “Characterizing the nonlinear behavior of a pseudoelastic oscillator via the wavelet transform”. *Proceedings of the Institution of Mechanical Engineers, Part C: Journal of Mechanical Engineering Science*, Vol. 230, No. 1, pp. 120–132.

Pust, L. and Peterka, F., 2003. “Impact oscillator with hertz’s model of contact”. *Meccanica*, Vol. 38, No. 1, pp. 99–116.

Pust, L., 1999. “Models of weak stops-application to 2dof system”. In *Proc. 10th World Congress on TMM*. Vol. 4, pp. 20–24.

Rao, S.S., 2007. *Vibration of continuous systems.* John Wiley & Sons.

Serweta, W., Okolewski, A., Blazejczyk-Okolewska, B., Czolczynski, K. and Kapitaniak, T., 2014. “Lyapunov exponents of impact oscillators with hertzŒ¸s s and newtonŒ¸s s contact models”. *International Journal of Mechanical Sciences*, Vol. 89, pp. 194–206.

Shaw, S.W. and Holmes, P., 1983. “A periodically forced piecewise linear oscillator”. *Journal of Sound and Vibration*, Vol. 90, No. 1, pp. 129–155.

Shi, J., Bamer, F. and Markert, B., 2018. “A structural pounding formulation using systematic modal truncation”. *Shock and Vibration*, Vol. 2018.

Stoianovici, D. and Hurmuzlu, Y., 1996. “A critical study of the applicability of rigid-body collision theory”. *Journal of Applied Mechanics*, Vol. 63, No. 2, pp. 307–316.

Stronge, W.J., 2004. *Impact mechanics.* Cambridge university press.

Stronge, W., 1991. “Unraveling paradoxical theories for rigid body collisions”. *Journal of Applied Mechanics*, Vol. 58, No. 4, pp. 1049–1055.

Varanis, M., Balthazar, J., Silva, A., Mereles, A. and Pederiva, R., 2018a. “Remarks on the sommerfeld effect characterization in the wavelet domain”. *Journal of Vibration and Control*, p. 1077546318771804.

Varanis, M., Mereles, A., Balthazar, J., Tusset, A. and Oliveira, C., 2017. “Impact dynamics models: a short review on nonlinearities effects”. *International Review of Mechanical Engineering (IREME)*, Vol. 11, No. 3.

Varanis, M., Mereles, A., Silva, A., Balthazar, J., Tusset, A. and Oliveira, C., 2018b. “Experimental evaluation of a vibro-impact model for two adjacent shear-building structures”. In *Procceedings 14th International Conference on Vibration Engineering and Technology of Machinery*. Journal of Vibration Engineering & Technologies.

Varanis, M., Mereles, A., Silva, A., Balthazar, J.M. and Tusset, Â.M., 2018c. “Rubbing effect analysis in a continuous rotor model”. In *International Conference on Rotor Dynamics*. Springer, pp. 387–399.

Veluswami, M. and Crossley, F., 1975. “Multiple impacts of a ball between two platesâA Tpart 1: Some experimental observations”. *Journal of Engineering for Industry*, Vol. 97, No. 3, pp. 820–827.

Vukobratovic, M.K. and Potkonjak, V., 1999. “Dynamics of contact tasks in robotics. part i: general model of robot ´interacting with environment”. *Mechanism and machine theory*, Vol. 34, No. 6, pp. 923–942.

Wagg, D. and Bishop, S., 2000. “A note on modelling multi-degree of freedom vibro-impact systems using coefficient of restitution models”. *Journal of Sound and vibration*, Vol. 236, No. 1, pp. 176–184.

Wang, J., Wang, H. and Wang, T., 2013. “External periodic force control of a single-degree-of-freedom vibroimpact system”. *Journal of Control Science and Engineering*, Vol. 2013, p. 13.

Wiercigroch, M. and Sin, V., 1998. “Experimental study of a symmetrical piecewise base-excited oscillator”. *Journal of Applied Mechanics*, Vol. 65, No. 3, pp. 657–663.

Wittenburg, J., 2013. *Dynamics of systems of rigid bodies*, Vol. 33. Springer-Verlag.

Zhang, L., Jiang, H. and Liu, Y., 2018. “Bifurcation analysis of a rigid impact oscillator with bilinear damping”. *Shock and Vibration*, Vol. 2018.